

# Restraining FOXO3-dependent transcriptional BMF activation underpins tumour growth and metastasis of E-cadherin-negative breast cancer

M Hornsveld<sup>1,3</sup>, M Tenhagen<sup>2,3</sup>, RA van de Ven<sup>2</sup>, AMM Smits<sup>1</sup>, MH van Triest<sup>1</sup>, M van Amersfoort<sup>2</sup>, DEA Kloet<sup>1</sup>, TB Dansen<sup>1</sup>, BM Burgering<sup>1</sup> and PWB Derksen<sup>\*,2</sup>

Loss of cellular adhesion leads to the progression of breast cancer through acquisition of anchorage independence, also known as resistance to anoikis. Although inactivation of E-cadherin is essential for acquisition of anoikis resistance, it has remained unclear how metastatic breast cancer cells counterbalance the induction of apoptosis without E-cadherin-dependent cellular adhesion. We report here that E-cadherin inactivation in breast cancer cells induces PI3K/AKT-dependent FOXO3 inhibition and identify FOXO3 as a novel and direct transcriptional activator of the pro-apoptotic protein BMF. As a result, E-cadherin-negative breast fail to upregulate BMF upon transfer to anchorage independence, leading to anoikis resistance. Conversely, expression of BMF in E-cadherin-negative metastatic breast cancer cells is sufficient to inhibit tumour growth and dissemination in mice. In conclusion, we have identified repression of BMF as a major cue that underpins anoikis resistance and tumour dissemination in E-cadherin-deficient metastatic breast cancer.

*Cell Death and Differentiation* (2016) 23, 1483–1492; doi:10.1038/cdd.2016.33; published online 1 April 2016

Development and homeostasis of glandular structures such as the mammary gland depend on spatiotemporal induction of apoptosis upon loss of cell–cell and cell–matrix attachment, a process known as anoikis.<sup>1,2</sup> Proper anoikis regulation ensures the formation of hollow lumen within a glandular epithelium structure by induction of apoptosis in selective non-polarised luminal epithelial cells that line the ductal structures.<sup>3,4</sup> In the mammary gland, the pro-apoptotic proteins BIM and BMF induce apoptosis upon cell detachment and as such contribute to the formation of mammary ductal lumen.<sup>5,6</sup>

Anoikis is regulated by an intricate regulation of the balance between pro-apoptotic and anti-apoptotic proteins.<sup>7</sup> Anti-apoptotic BCL-2 family proteins (BCL-2, BCL-xL and MCL1) compete with the pro-apoptotic molecules (BIM, PUMA, NOXA, BID, BAD or BMF) for binding to BAK and BAX to prevent mitochondrial membrane permeabilisation and subsequent apoptosis. Expression of pro-apoptotic proteins can be induced by a variety of stresses, including DNA damage, nutrient deprivation, heat and hypoxia.<sup>8</sup> BMF appears to specifically function to induce anoikis in epithelial cells.<sup>5,9</sup> It is, however, still controversial whether activation of factors such as BMF is induced through transcriptional activation or by posttranslational events in the cytosol.<sup>10</sup>

Correct execution of apoptosis in luminal mammary cells is deregulated during the early stages of breast cancer, such as atypical hyperplasia and ductal carcinoma *in situ*, resulting in filling of the mammary duct with anoikis-resistant cells.<sup>11</sup>

Several studies have shown that activation of oncogenic growth factor receptor (GFR) signalling can induce aberrant filling of the luminal space.<sup>3,5,12</sup> Similar effects have been observed upon inhibition of pro-apoptotic players such as BIM, BMF and p53,<sup>5,6,13</sup> indicating that either GFR activation and/or the inhibition of distal pro-apoptotic effectors underlie anchorage independence of breast cancer cells. Indeed, mutations in the PI3K and p53 pathway are among the most observed mutations in epithelial cancers, including breast cancer.<sup>14</sup> Moreover, hyperactivation of PI3K and its downstream effector AKT/PKB can lead to repression of apoptosis through phosphorylation-dependent inactivation of pro-apoptotic proteins, such as BAD.<sup>5,15,16</sup>

Enhanced growth factor signalling can also be induced through downregulation of the epithelial adherens junction (AJ).<sup>17,18</sup> E-cadherin is the core component of the AJ and a master regulator of epithelial integrity, linking the cell membrane to the cytoskeleton.<sup>19</sup> Although loss of E-cadherin in the mammary gland is not tolerated,<sup>20–22</sup> mammary-specific E-cadherin inactivation following loss of p53 in mice leads to the acquisition of anoikis resistance of tumour cells and subsequent dissemination, demonstrating E-cadherin loss as a prerequisite for metastatic disease progression.<sup>23</sup>

Despite its repression by growth factor signals, the apoptotic machinery is functionally intact in cancer cells. Targeting the apoptotic machinery has become increasingly interesting in cancer therapy, as intervention strategies using novel

<sup>1</sup>Department of Molecular Cancer Research, University Medical Center Utrecht, Utrecht, The Netherlands and <sup>2</sup>Department of Pathology, University Medical Center Utrecht, Utrecht, The Netherlands

\*Corresponding author: PWB Derksen, Department of Pathology, University Medical Center Utrecht, H04.312, Heidelberglaan 100, Utrecht, CX 3584, The Netherlands. Tel: +31 88 7568086; E-mail: pderksen@umcutrecht.nl

<sup>3</sup>These authors contributed equally to this work.

**Abbreviations:** GFR, growth factor receptor; AJ, adherens junction; Ad, adherent; Sus, suspension; FACS, fluorescent-activated cell sorting; ChIP, chromatin immunoprecipitation; iBMF, inducible BMF; iFOXO, inducible FOXO3; Dox, doxycycline

Received 10.8.15; revised 24.2.16; accepted 01.3.16; Edited by C Borner; published online 01.4.2016

BH-3-only protein mimetic compounds in combination with dual specificity inhibitors of PI3K and mTOR have shown promising results.<sup>24,25</sup> Here we have identified *BMF* as a direct transcriptional target of FOXO3 in breast cancer cells. Our data show that FOXO-dependent *BMF* expression is repressed in E-cadherin-negative and metastatic breast cancer cells and that expression of *BMF* is sufficient to inhibit tumour growth and dissemination in mice. We have thereby linked loss of E-cadherin to a cell intrinsic inhibition of *BMF*-dependent anoikis, a crucial step in malignant tumour progression.

## Results

**Anoikis-resistant breast cancer cells restrain the expression of *BMF*.** To identify the proteins that control anchorage independence of metastatic breast cancer cells, we cultured E-cadherin-expressing anchorage-dependent and anoikis-resistant E-cadherin-negative breast cancer cells from mouse and human origin in suspension (Sus). Under these conditions, the non-metastatic mouse mammary carcinoma cell line Trp53<sup>Δ/Δ</sup>-4 and human MCF7 underwent anoikis as previously demonstrated.<sup>20,26</sup> In contrast, mouse and human E-cadherin-negative mILC1 and MDA-MB-231 cells were anoikis resistant (Figures 1a and b).

To determine which of the key anti-apoptotic and pro-apoptotic molecules were induced during anoikis, we assayed the protein and mRNA expression levels of the anti-apoptotic family members *BCL2*, *BCL-XL* and *MCL1* and the pro-apoptotic *NOXA*, *PUMA*, *BIM*, *BID* and *BMF*. We observed that all cell lines upregulated *BCL2* protein levels and showed increased *BID* cleavage under anchorage-independent conditions regardless of E-cadherin status. For *NOXA* and *PUMA*, no changes were detected in protein levels (Supplementary Figure S1A). In line with previous findings,<sup>5,6,27</sup> we detected a clear induction of *BIM* and *BMF* in the anoikis-sensitive Trp53<sup>Δ/Δ</sup>-4 and MCF7 (Figures 1c and d, Supplementary Figures S1B and C). In contrast, the metastatic cell lines mILC1 and MDA-MB-231 did not show a comparable upregulation of either *BIM* or *BMF* (Figures 1c and d, Supplementary Figures S1B and C). Subsequent quantitative PCR experiments demonstrated that the only pro-apoptotic gene that was transcriptionally upregulated in both mouse and human E-cadherin-expressing anchorage-independent cells was *BMF* (Figures 1e and f and Supplementary Figures S2A and B). We observed that, although E-cadherin-negative cells induced *BMF* under anchorage-independent conditions, the expression levels were 3–10-fold lower relative to Trp53<sup>Δ/Δ</sup>-4 and MCF7. These data demonstrate that anchorage-independent E-cadherin-negative cells restrain transcriptional upregulation of *BMF*, a key inducer of anoikis.

Despite the fact that *BMF* is the major pro-apoptotic factor that showed uniform transcriptional upregulation in suspension settings, at the protein level both *BMF* and *BIM* are increased (Figures 1c and d and Supplementary Figures S1B and C). To determine whether these two BH3-only factors are specifically required to induce anoikis, we performed loss-of-function studies and assessed the effect of *BMF* and/or *BIM* loss on anoikis resistance of mouse and human E-cadherin-positive cells. Using two independent targeting sequences, we

induced knockdown and observed that loss of either *BMF* or *BIM* led to a significant increase in anoikis resistance of Trp53<sup>Δ/Δ</sup> and MCF7 cells (Figures 2a–f). Concomitant knockdown of *BMF* and *BIM* also resulted in a significant increase in anoikis resistance when compared with controls (Figures 2a–f). Overall, our data does not indicate that dual inhibition of *BMF* and *BIM* has an additive effect when compared with the single *BMF* knockdown experiments (Figures 2a and b). In short, our data demonstrate that *BMF* and *BIM* both contribute to the induction of anoikis in E-cadherin-positive breast cancer cells. Further, our data indicate that *BMF* and *BIM* are non-redundant and have overlapping functions in the regulation of anoikis of E-cadherin-expressing cells. Overall, we show that *BIM* and *BMF* expression is increased upon transfer to anchorage-independent conditions to induce anoikis. However, our data indicate that, in contrast to *BIM*, the upregulation of *BMF* under these conditions is transcriptionally regulated.

**Loss of E-cadherin results in anoikis resistance and restricts *BMF* expression.** To determine whether E-cadherin loss is causal to the repression of *BMF* expression in breast cancer, we generated E-cadherin knockout cell lines using the CRISPR/Cas9 system. Guide RNAs targeting the E-cadherin locus were expressed in Trp53<sup>Δ/Δ</sup> and MCF7 cells, which were subsequently fluorescent-activated cell sorted (FACS) based on E-cadherin expression, resulting in E-cadherin-negative cell lines. In contrast to control cells, the E-cadherin knockout cell lines failed to establish E-cadherin-based cell–cell junctions and consequently grew dispersed as solitary cells (Figure 3a). As expected, we observed that E-cadherin loss in mouse and human cells resulted in the acquisition of anoikis resistance (Figure 3b). Importantly, we noted a significant reduction of *BMF* expression in E-cadherin knockout cell lines relative to control cells upon transfer to anchorage independence (Figures 3c and d). These results confirm that loss of E-cadherin is causal to the acquisition of anoikis resistance and show that loss of E-cadherin leads to transcriptional repression of *BMF* expression upon loss of cell–matrix attachment.

***BMF* expression is inhibited by growth factor signalling-dependent repression of FOXO3.** Because *BMF* was transcriptionally regulated upon transfer to anchorage independence, we hypothesised that either direct transcription repression or inhibition of a transcription factor could underlie the differential *BMF* expression in anoikis-resistant breast cancer cells. We therefore analysed the human genomic *BMF* promoter region and identified two FOXO consensus-binding sites (*TTGTTTA*). FOXOs are directly regulated and suppressed by canonical PI3K/AKT signalling and known transcription factors for the pro-apoptotic genes *BIM*, *NOXA* and *PUMA*.<sup>28</sup>

To assess whether *BMF* is a direct FOXO target, we performed a chromatin immunoprecipitation (ChIP) with the most ubiquitously expressed FOXO transcription factor, FOXO3. To this end, we stably introduced a doxycycline (Dox)-inducible FOXO3 (iFOXO) construct in MCF7 cells and performed ChIP in the presence of the allosteric inhibitor VIII (AKTi) to prevent upstream inhibition of FOXO3 by AKT. In line with the predicted binding sites, we noticed binding of FOXO3

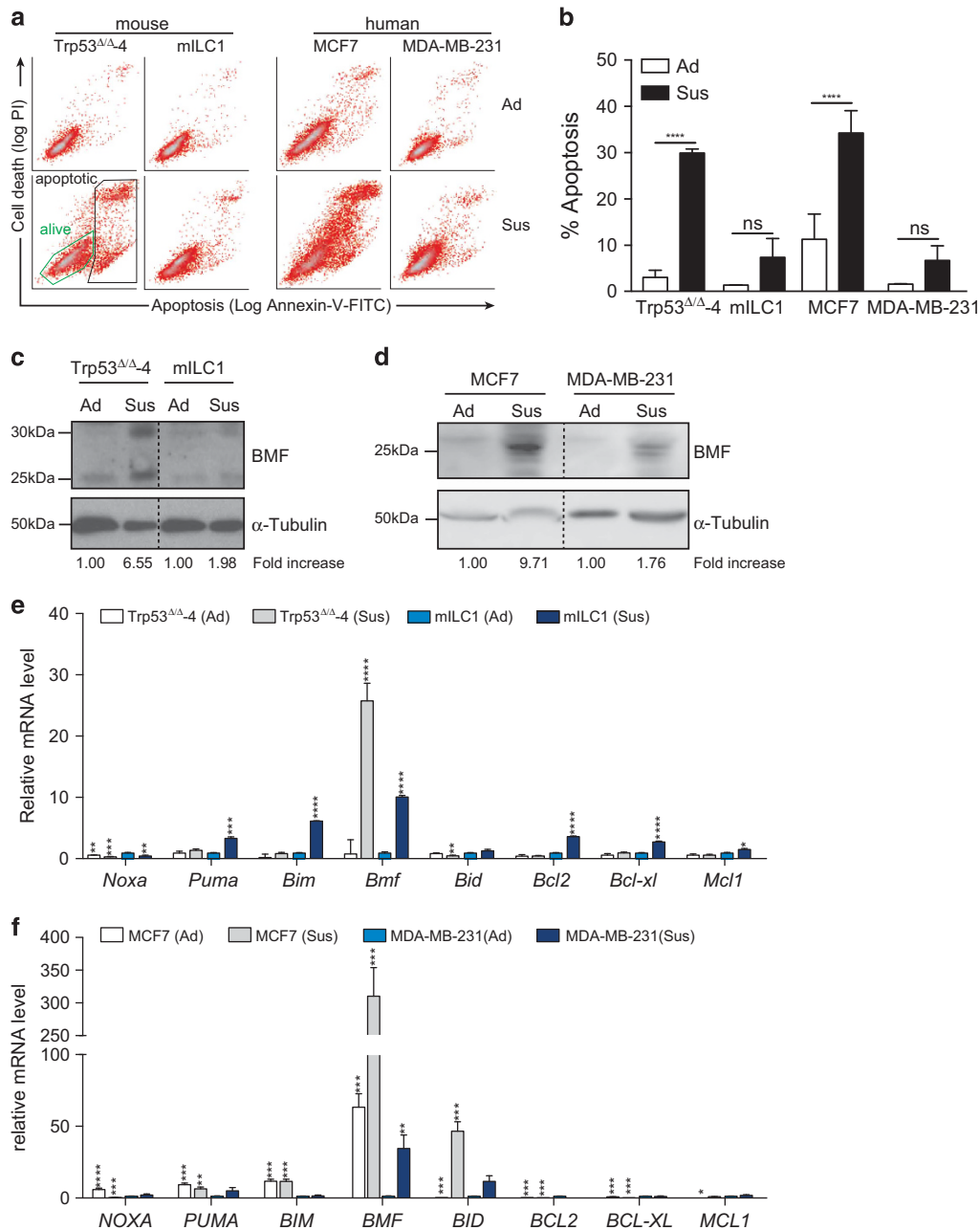


**Figure 1** Anchorage-independent E-cadherin-negative breast cancer cells restrain *BMF* expression. (a) Anoikis resistance in the E-cadherin-negative breast cancer cell lines mILC1 and MDA-MB-231. Shown are flow cytometric analyses of apoptosis and cell death using Annexin-V-FITC (fluorescein isothiocyanate) and propidium iodide after 24-h adherent (Ad) and suspension (Sus) conditions. Note the robust induction of anoikis in the E-cadherin-expressing cells Trp53 $\Delta\Delta$ -4 and MCF7. (b) Quantification of anoikis induction measured by flow cytometry in panel (a). Data represent mean  $\pm$  S.D.,  $n=3$ ,  $t$ -test  $*P<0.05$ ,  $**P<0.005$ ,  $***P<0.0005$ . (c and d) Western blotting analysis of *BMF* and  $\alpha$ -Tubulin protein levels in Trp53 $\Delta\Delta$ -4 and mILC1. Blots are cropped in correspondence to the black box (c) and MCF7 and MDA-MB-231 cells grown under Ad and Sus conditions. Blots are cropped corresponding to the black box. (e and f) Quantitative PCR analysis of *Noxa*, *Puma*, *Bim*, *Bmf*, *Bid*, *Bcl2*, *Bcl-xl* and *Mcl1* mRNA expression in Trp53 $\Delta\Delta$ -4 and mILC1 and MCF7 and MDA-MB-231 cultured in Ad and Sus culture. Data are relative to mRNA levels in Ad mILC1 cells (e) or MDA-MB-231 cells (f). Data represent the mean  $\pm$  S.D.,  $n=3$ ,  $t$ -test  $*P<0.05$ ,  $**P<0.005$ ,  $***P<0.0005$

to both consensus sites in the *BMF* promoter (Figure 4a). We confirmed these results by analysing induction of *BMF* upon expression of a dominant active form of FOXO3 (FOXO3.A3)<sup>29</sup> and showing that administration of Dox indeed resulted in a robust induction of *BMF* mRNA and protein levels upon FOXO3 activation (Figures 4c and d, Supplementary Figures S3A–C and S4A and B).

To determine whether FOXO3 activation was sufficient to induce anoikis in E-cadherin-negative cells, we cultured mILC1-iFOXO3.A3 and MDA-MB-231-iFOXO3.A3 in suspension and assayed anchorage-independent survival. Addition of Dox triggered anoikis in mILC1 (Figure 4b), confirming that FOXO activation is indeed sufficient to prevent anchorage independence in E-cadherin-negative breast cancer cells.

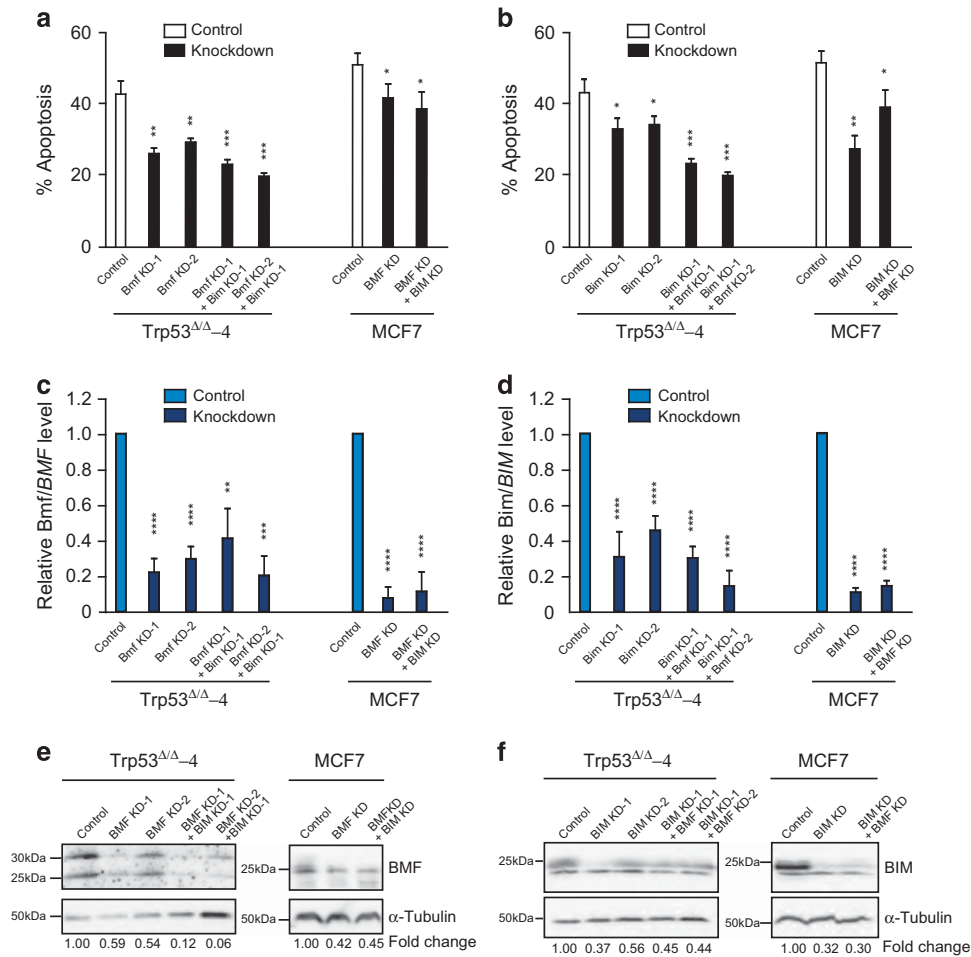


**Figure 2** Loss of *BMF* or *BIM* increases anoikis resistance of E-cadherin-expressing breast cancer cells. **(a and b)** Knockdown of *BMF* and *BIM* reduces apoptosis of Trp53<sup>Δ/Δ</sup> and MCF7 cells cultured in Sus. Flow cytometric quantifications of apoptosis using Annexin-V-FITC (fluorescein isothiocyanate) and propidium iodide after 24 h in Sus culture. **(c and d)** Quantitative PCR analysis of *BMF* and *BIM* mRNA knockdown efficiency. Data represent the mean  $\pm$  S.D.,  $n=3$ ,  $t$ -test \* $P<0.05$ , \*\* $P<0.005$ , \*\*\* $P<0.0005$ , \*\*\*\* $P<0.0005$ . **(e and f)** Western blotting analysis of *BMF* and *BIM* protein levels shows successful *BMF* and *BIM* knockdown in Trp53<sup>Δ/Δ</sup> and MCF7 cells cultured in Sus. Blots are cropped corresponding to the black box

Although MDA-MB-231-iFOXO3.A3 cells showed a modest increase in *BMF* expression upon expression of FOXO3 (Supplementary Figure S4B), this did not lead to anoikis, which indicates that the induced *BMF* levels were insufficient to cause apoptosis in these anchorage-independent breast cancer cells.

Activation of the PI3K/AKT pathway by GFR signalling and ectopic expression of either oncogenic PI3K<sup>E545K</sup> or myristoylated AKT1 results in repression of anoikis in mammary epithelial cells.<sup>5</sup> Interestingly, we have previously shown that inactivation of E-cadherin function in cancer cells results in hypersensitisation of GFR signalling without activating mutations.<sup>18</sup> To confirm that active PI3K/AKT signalling, which is an established upstream inhibitor of FOXO, controls anoikis resistance, we cultured mILC1 cells and the MCF7- $\Delta$ CDH1 cells in suspension and inhibited AKT activation using AKTi, and observed that AKTi resulted in a twofold increase in anoikis (Figures 5a and b). More important, we could show that AKT inhibition resulted in a 2–3-fold upregulation of *BMF* mRNA and protein expression in anchorage-independent cells (Figures 5c–e).

In conclusion, our data show that E-cadherin-negative metastatic breast cancer cells restrain anoikis through PI3K/AKT signalling, a cue that subsequently inhibits FOXO3-dependent transcriptional activation of its pro-apoptotic target *BMF*.

**Upregulation of *BMF* expression restrains anchorage-independent tumour growth and metastasis of E-cadherin-negative mammary cancer in mice.** Because *BMF* was the major pro-apoptotic factor upregulated in anoikis-sensitive breast cancer cell lines, we determined whether induction of *BMF* expression was sufficient to induce anoikis in E-cadherin-negative breast cancer cells. To this end, we stably introduced a Dox-inducible *BMF* cDNA expression system (iBMF) in mILC1 and MDA-MB-231 cells (Figure 6a) and assayed anoikis resistance. Expression of *BMF* was indeed sufficient to cause a marked increase in apoptosis in both cell types (Figures 6b and c). Moreover, treating mILC1 and MDA-MB-231 cells with increasing concentrations of the BH3-mimetic drug ABT-199 induced a dose-dependent execution of apoptosis (Figure 6d),

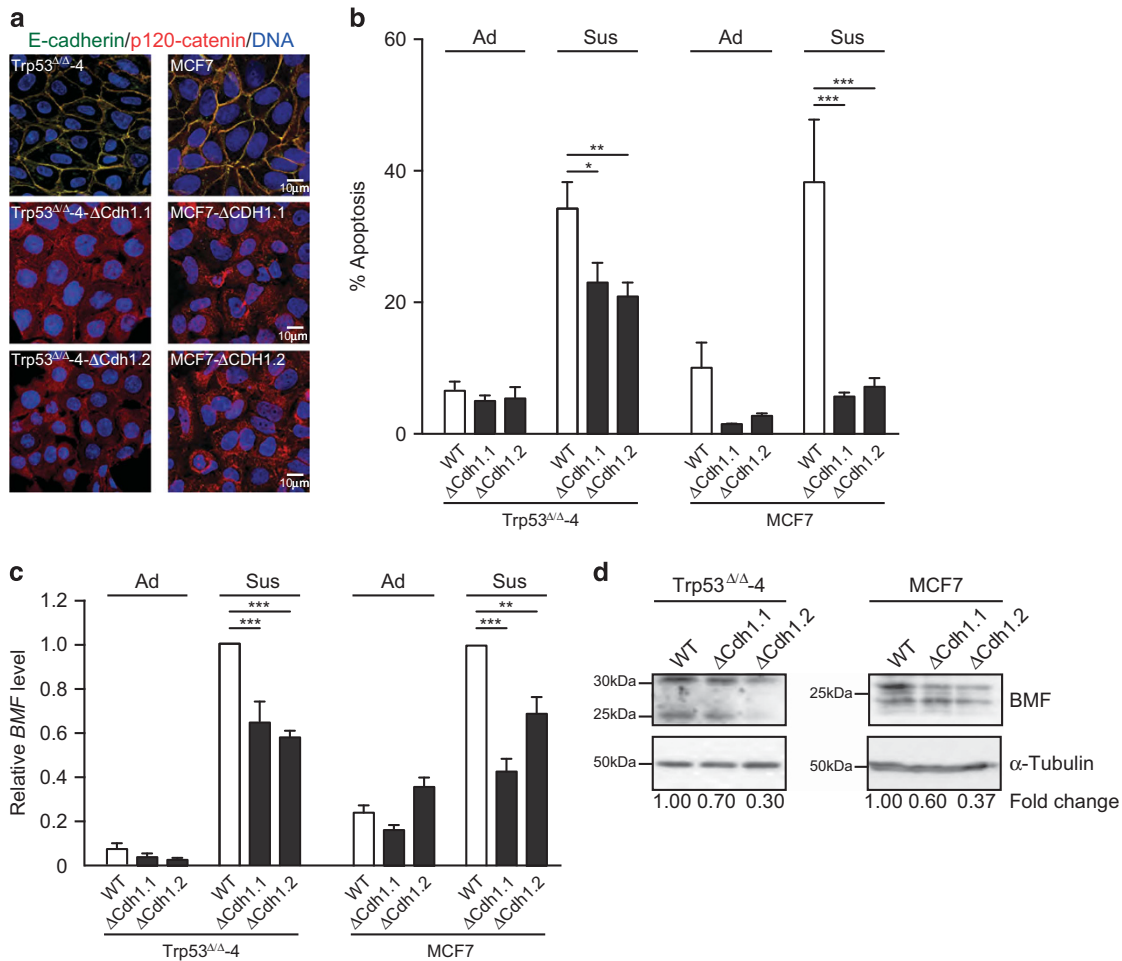


**Figure 3** Loss of E-cadherin results in anoikis resistance and repression of BMF expression. (a) Immunofluorescence analysis of Trp53<sup>ΔΔ</sup> and MCF7 cells targeted with E-cadherin-specific gRNA. ΔCDH1.1 and ΔCDH1.2 cells grow dispersed, show loss of E-cadherin (Green) and cytoplasmic translocation of p120-catenin (Red) and fail to establish cell–cell junctions. (b) Acquisition of anoikis resistance upon loss of E-cadherin in Trp53<sup>ΔΔ</sup> and MCF7 cells. Shown are quantifications of flow cytometry analyses of apoptosis and cell death using Annexin-V-FITC (fluorescein isothiocyanate) and propidium iodide after 24 h in Ad and Sus culture. Data represent mean ± S.D., *n* = 3, *t*-test \**P* < 0.05, \*\**P* < 0.005, \*\*\**P* < 0.0005. (c) BMF is repressed in E-cadherin knockout Trp53<sup>ΔΔ</sup> and MCF7 cells. Quantitative PCR analysis shows *Bmf* or *BMF* expression after 24 h in Ad and Sus culture conditions. Data are relative to mRNA levels in Sus cells. Data represent the mean ± S.D., *n* = 3, *t*-test \*\*\**P* < 0.005, \*\*\*\**P* < 0.0005. (d) Western blotting analysis shows increased BMF protein expression in Trp53<sup>ΔΔ</sup> and MCF7 cells cultured in Sus. Blots are cropped corresponding to the black box

suggesting that anchorage-independent E-cadherin-deficient breast cancer cells have a lower threshold for the BH3-only protein-dependent execution of anoikis. Together, these results show that increased levels of BMF or inhibition of BCL2 using the BMF-mimetic ABT-199 is sufficient to induce apoptosis in E-cadherin-negative cells, especially in an anchorage-independent setting.

As anoikis resistance is an excellent prognosticator of E-cadherin-negative breast cancer growth and metastasis,<sup>20,23</sup> we investigated the effect of BMF expression on tumour growth *in vivo*. To this end, we orthotopically transplanted 10,000 mILC1 cells carrying either an empty vector or the iBMF expression vector in recipient mice and monitored tumour growth. Once tumours reached an average volume of 100 mm<sup>3</sup>, we induced BMF expression by feeding mice Dox-containing chow. Treatment of mILC1 cells carrying the empty expression vector with Dox either at a 100 mm<sup>3</sup> or when metastasis was detected using bioluminescence imaging (BLI) did not result in significant changes in tumour growth

(Figure 7a). In contrast, BMF expression induced a significant reduction in tumour growth (Figure 7b). Moreover, induction of BMF expression when metastases were detected led to a robust 19-fold decrease in primary tumour volume (Figure 7c). Importantly, we observed a reduction in metastasis formation based upon BMF expression on thoracic BLI in Dox-fed mice when compared with control mice (Figures 7d–h).

In closing, our data establish that restriction of FOXO3-dependent BMF expression underpins anchorage-independent tumour growth and metastasis of E-cadherin-negative breast cancer cells.

## Discussion

Acquisition of anchorage independence through evasion of apoptosis is a hallmark of cancer.<sup>30</sup> Metastatic cells have shifted the regulation of pro-apoptotic and anti-apoptotic mechanisms toward survival and have thereby gained the possibility to bypass the induction of anoikis during dissemination.

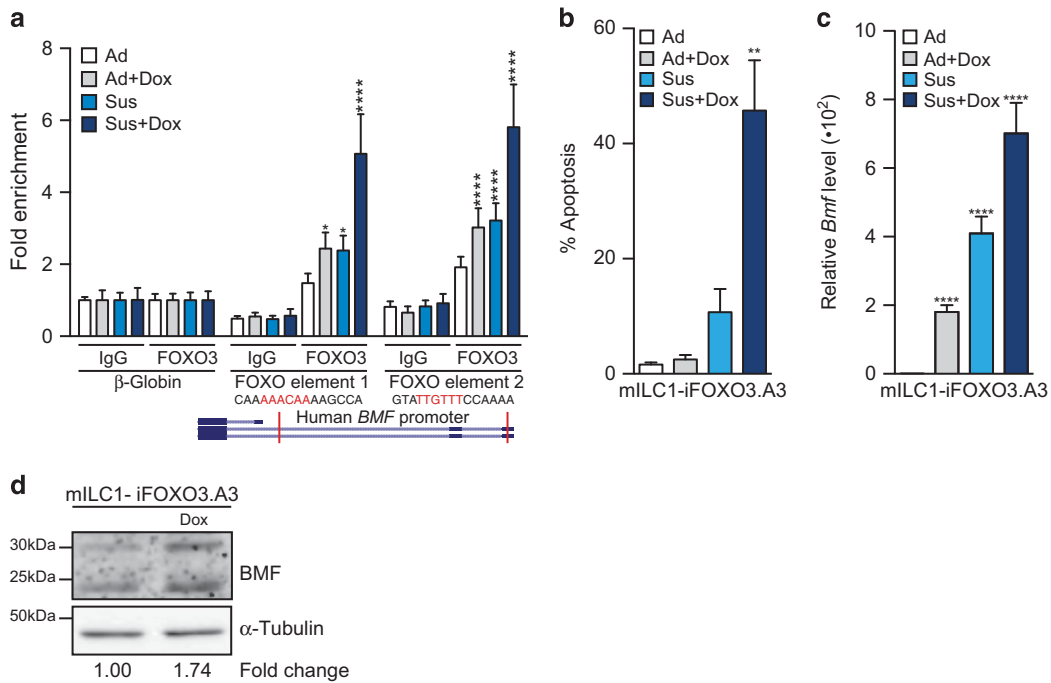


**Figure 4** *BMF* is a direct FOXO3 target gene in breast cancer cells. (a) *BMF* is a direct FOXO3 target. FOXO3 binds the *BMF* promoter after AKT inhibition and during anchorage-independent growth. Average enrichment in *BMF* promoter chromatin recovery after FOXO3-ChIP in MCF7 growing under Ad, Sus and upon FOXO3 expression in Ad and Sus conditions (Ad+Dox, Sus+Dox, respectively). Data represent mean  $\pm$  S.D., *t*-test  $n=3$ , \* $P<0.05$ , \*\*\*\* $P<0.00005$ . (b) Activation of FOXO induces anoikis. Quantification of anoikis in mILC1-iFOXO3.A3 measured by flow cytometry, data represent mean  $\pm$  S.D.,  $n=3$ , *t*-test \*\* $P<0.005$ . (c and d) FOXO3 activation induces *BMF* expression in mILC1. Shown are relative mRNA and protein levels in Sus upon FOXO3.A3 expression in mILC1 cells. Blots are cropped corresponding to the black box

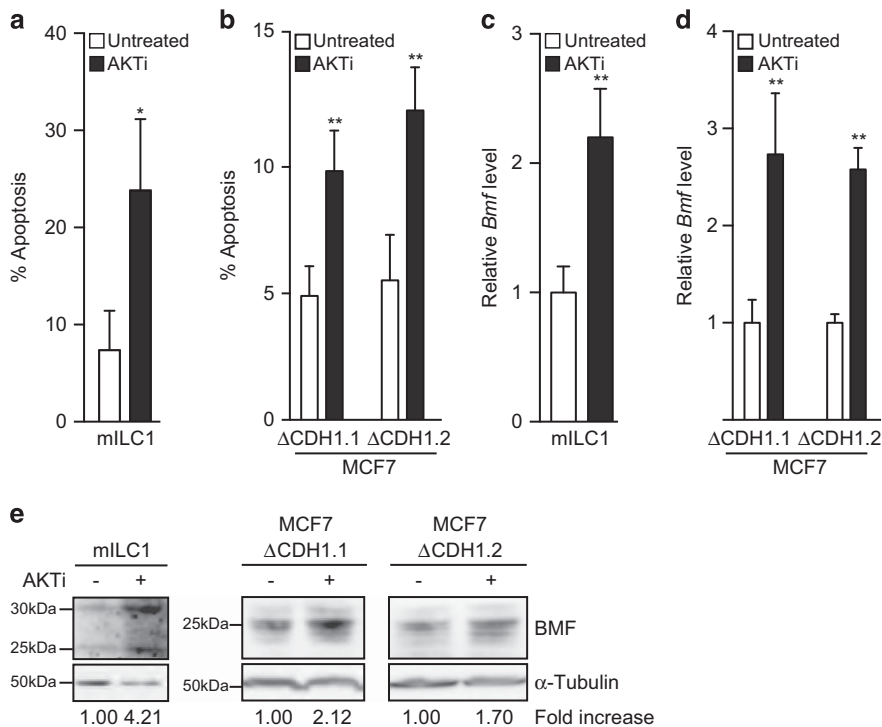


**Figure 5** GFR signals restrain *BMF* expression through PI3K/AKT-dependent signals. (a and b) Anoikis resistance in E-cadherin-negative breast cancer cells is AKT dependent. Shown is the quantification of anoikis induction in mILC1, MCF7- $\Delta$ CDH1.1 and MCF7- $\Delta$ CDH1.2 grown in Sus measured by flow cytometry. Data represent the mean  $\pm$  S.D.,  $n=3$ , *t*-test \* $P<0.05$ , \*\* $P<0.005$ . (c-e) AKT inhibition results in *BMF* expression. Shown are quantitative PCR analyses of *Brmf*/*BMF* mRNA and western blotting analyses of *Brmf*/*BMF* protein levels in mILC1, MCF7- $\Delta$ CDH1.1 and MCF7- $\Delta$ CDH1.2 cultured in Sus and after treatment with AKTi. Data represent the mean  $\pm$  S.D.,  $n=3$ , *t*-test \* $P<0.05$ , \*\* $P<0.005$ . Blots are cropped corresponding to the black box

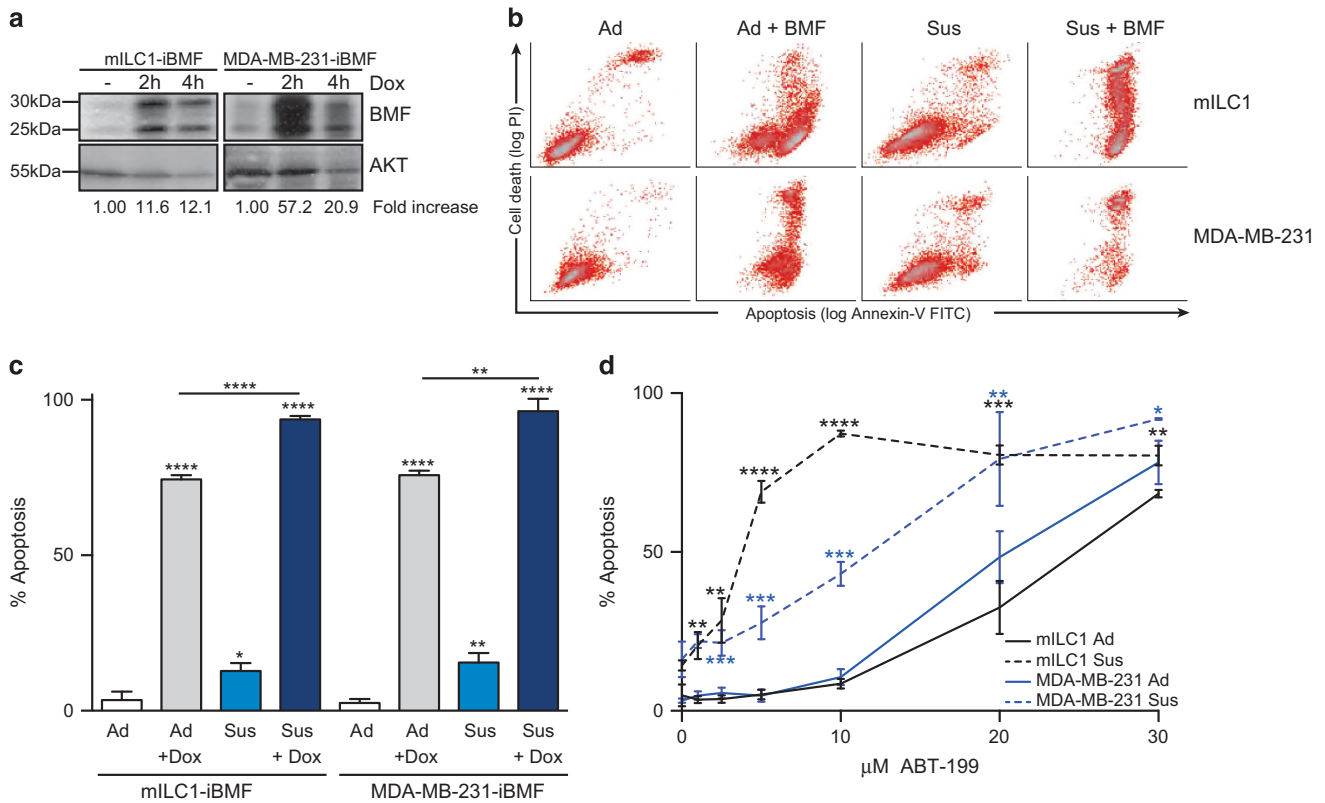


**Figure 6** BMF expression is sufficient to induce apoptosis in E-cadherin-negative breast cancer cells. (a) Inducible expression of BMF in mILC1-iBMF and MDA-MB-231-iBMF before and after Dox treatment. Blots are cropped corresponding to the black box. (b and c) BMF expression induces apoptosis in mILC1 and MDA-MB-231 cells. Flow cytometric analysis of anoikis induction by Annexin-V-FITC (fluorescein isothiocyanate) and propidium iodide staining of mILC1-iBMF and MDA-MB-231-iBMF cells (b). (c) Depicts a quantification of the anoikis induction of mILC1-iBMF and MDA-MB-231-iBMF measured in panel (b). Data represent mean  $\pm$  S.D.,  $n=3$ ,  $t$ -test  $*P < 0.05$ ,  $**P < 0.005$ ,  $***P < 0.0005$ ,  $****P < 0.00005$ . (d) Induction of apoptosis and anoikis by the BMF mimetic ABT-199. FACS analysis of apoptosis induction using Annexin-V-FITC and propidium iodide staining of mILC1 and MDA-MB-231 cells after 24 h of treatment with ABT-199 in Ad and Sus conditions. Data represent mean  $\pm$  S.D.,  $n=3$ ,  $*P < 0.05$ ,  $**P < 0.005$ ,  $***P < 0.0005$ ,  $****P < 0.00005$

Activation of growth factor signalling in cancer cells is essential for anoikis resistance owing to modulation of expression and activity of apoptotic factors.<sup>25</sup> Others and we have demonstrated that inactivation of E-cadherin underpins anoikis resistance in breast cancer cells, a finding that appears to depend on hyper-sensitisation of GFR signalling through AKT/PKB and ERK upon dismantling of the AJ complex.<sup>17,18,20,23,31</sup> As these mechanisms confer constitutive activation of GFR signals in breast cancer cells, it provides a clear rationale for the maintenance of anoikis resistance in E-cadherin-deficient breast cancer cells. Although AKT/PKB and ERK can control the posttranslational modulation of BAD, BIM and BAX, our current data show that anoikis-resistant breast cancer cells restrain *BMF* transcription, the main pro-apoptotic factor uniformly expressed in E-cadherin-expressing breast cancer cells upon transfer to anchorage independence.<sup>15,16,32</sup> Elegant studies by the Brugge laboratory have identified BIM and BMF as key anoikis regulators of luminal mammary cells, a process counterbalanced by constitutive activation of growth factor-induced PI3K/AKT pathways.<sup>5,6</sup> However, the underlying mechanism that prevented metastatic breast cancer cells from expressing *BMF* upon loss of anchorage remained unclear. As we detected clear changes in *BMF* mRNA levels upon transfer to anchorage

independence when comparing breast cancer cells in the context of E-cadherin expression, we probed for transcriptional upstream cues, which resulted in our finding that FOXOs are key players in the regulation of *BMF* expression in breast cancer.

BMF can directly compete for BAK/BAX binding with BCL2 and thereby drive apoptosis. Our data indicate that the increase in BMF expression, rather than the levels of BCL2, is the rate-limiting factor driving breast cancer cell survival. First, the robust upregulation in *BMF* mRNA expression in anoikis-sensitive cells combined with reduced *BMF* expression in anoikis-resistant cells led us to think that a specific BMF threshold should be reached to induce anoikis. Second, although anoikis-resistant cells induced *BMF* transcription in the absence of anchorage, this did not trigger anoikis, despite expressing comparable levels of BCL2 when compared with anoikis-sensitive cells. In line with this, we did not detect differences in the expression levels of BCL2 upon transfer to anchorage independence between cell lines. Finally, we could force anoikis-resistant cells to undergo apoptosis by ectopic expression of BMF or treatment with ABT-199. Together, our data show that loss of the AJ leads to GFR-induced signals that block FOXO-dependent BMF expression, a feature that is essential for survival in breast cancer cells during metastasis.

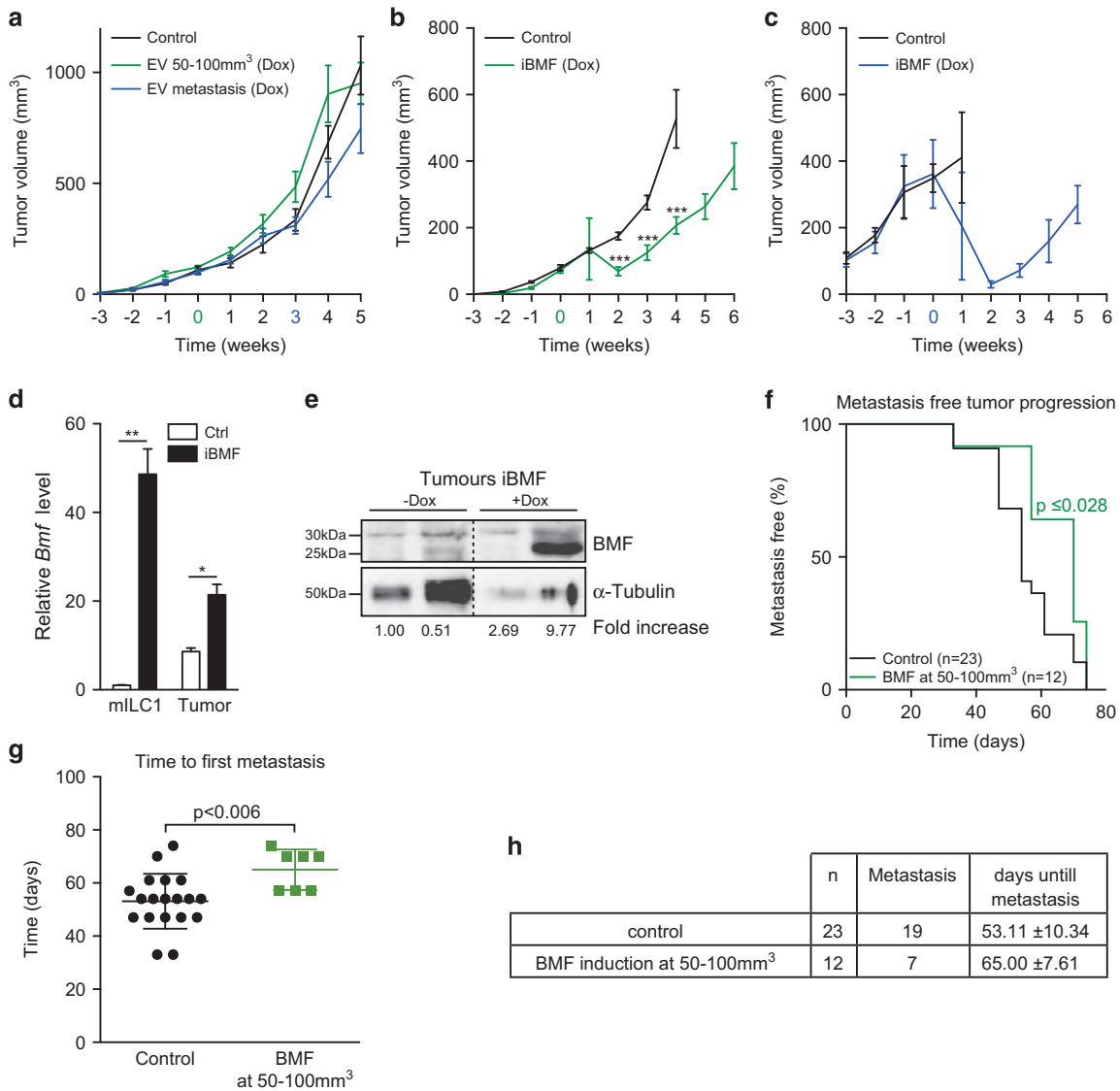


**Figure 7** *BMF* expression restrains anchorage-independent tumour growth and metastasis of E-cadherin-negative breast cancer cells. (a) Dox treatment does not influence tumour growth of mILC1 cells carrying the empty Dox-inducible expression vector (EV). (b) *BMF* expression inhibits mammary tumour growth in mice. Primary tumour growth of control mice ( $n = 10$ ) and mice treated with Dox ( $n = 12$ ), which was started when tumours reached a volume of 100 mm<sup>3</sup>. Data represent the mean tumour volume  $\pm$  S.E.M., Holm-Sidak corrected  $t$ -test  $***P < 0.0005$ . (c) *BMF* expression inhibits mammary tumour growth in mice with metastatic disease. Primary tumour growth of control ( $n = 10$ ) and mice treated with Dox ( $n = 13$ ), which was started when lung metastasis were detected by BLI ( $> 2 \times 10^3$  photons/s/cm<sup>2</sup>/sr), data represent the mean tumour volume  $\pm$  S.E.M. (d) Successful *BMF* expression after Dox treatment was determined by quantitative PCR analysis of the parental mILC1-iBMF and in primary tumours derived from either untreated or Dox-treated mice. Data represent mean  $\pm$  S.D.,  $n = 3$ ,  $t$ -test  $*P < 0.05$ ,  $P < 0.005$ . (e) Western blotting analysis of tumour lysates shows *Bmf* induction upon Dox treatment of mice. Two untreated ( $-$  Dox) and treated ( $+$  Dox) tumours are shown, respectively. (f) *BMF* expression inhibits metastasis formation of mILC1 cells. Kaplan-Meier curve representing metastasis-free tumour progression measured in days until metastasis were detected by BLI in control mice ( $n = 23$ ) and mice treated with Dox at a primary tumour volume of 50–100 mm<sup>3</sup> ( $n = 12$ ), Mantel-Cox test  $P = 0.028$ . (g and h) Time until first metastasis are detected by BLI in control mice ( $n = 19$ ) and mice treated with Dox at a primary tumour volume of 50–100 mm<sup>3</sup> ( $n = 7$ ). Data represent individual mice with detected metastasis ( $> 2 \times 10^3$  photons/s/cm<sup>2</sup>/sr)  $\pm$  S.D., Welch's corrected  $t$ -test  $P < 0.0062$

Our results indicate that FOXO-dependent transcription of *BMF* may be subject of epigenetic regulation as well. Although we have ectopically activated FOXO3 under anchorage-dependent and -independent conditions, we detected further enhanced FOXO3 binding at the *BMF* promoter in suspension. The chromatin state of the *BMF* locus is expected to influence FOXO3 binding, as it is known that FOXO3 prefers to bind genomic regions associated with activating epigenetic marks.<sup>33,34</sup> Histone deacetylase (HDAC) activity has been

reported as a negative regulator of *BMF* expression, because inhibition of HDACs results in *BMF* expression in multiple human cancer cell lines.<sup>35,36</sup> How *BMF* is regulated posttranscriptionally remains to be fully characterised, but it was previously described that phosphorylation of ERK2 can inactivate *BMF* function.<sup>37,38</sup> In line with these findings, complementing HDAC inhibition with inhibitors of mitogenic signalling, that is, B-RAF, augments the pro-apoptotic effect of *BMF*.<sup>39</sup> This might also explain why *BMF* induction does not



directly lead to apoptosis in anchorage-independent MDA-MB-231 cells that show a constitutively elevated growth factor signalling owing to oncogenic KRAS and B-RAF mutations.<sup>40</sup>

Loss of BMF has been linked to tumour suppression in several cancer types.<sup>41</sup> Preclinical intervention strategies using BH3-only mimetics as monotherapy have been successful but mostly in lymphoid malignancies.<sup>42,43</sup> Recent studies indicated that BH3-mimetics can be used to treat non-lymphoid cancers but mostly in combination with oestrogen antagonists, proteasome inhibitors, specific PI3K-mTOR inhibitors or chemotherapy.<sup>24,44–49</sup> As previous findings from our laboratory demonstrated that E-cadherin-negative lobular breast cancer depends on p120-catenin-mediated activation of RhoA, Rock and subsequent actomyosin contraction,<sup>26</sup> we anticipate that dual inhibition of these pathways might be successful in E-cadherin-negative cancers that are not driven by oncogenic activation of GFR pathways. Although we do not yet know whether RhoA–Rock signals converge onto the GFR–AKT–FOXO axis in the regulation of anoikis resistance, the fact that FOXO expression had no effect on survival of B-RAF/KRAS-mutated MDA-MB-231 cells seems to be in line with this assumption. Moreover, given that human invasive lobular carcinoma mostly expresses ER and responds to oestrogen antagonists, our findings provide an additional option to improve current treatment regimens in lobular breast cancer by using a combination BH3-mimetics and ER-targeted drugs.

In conclusion, we have linked activation of GFR pathways to inhibition of FOXO3-dependent BMF expression and the regulation of anchorage-independent tumour growth and metastasis in E-cadherin-negative metastatic breast cancer cells.

## Materials and Methods

**Cell lines.** Mouse breast cancer cell lines *Trp53<sup>Δ/Δ</sup>-4* (KP8) and *mLc1* (KEP1) were derived from tumours that developed in female *K14cre;Trp53<sup>F/F</sup>* and *K14cre;Cdh1<sup>F/F</sup>;Trp53<sup>F/F</sup>* mice and cultured as described previously.<sup>23</sup> Human breast cancer cell lines MCF7 and MB-MDA-231 were verified by STR analysis and cultured as described.<sup>18</sup>

**Constructs, lentiviral transduction and transfections.** Lentiviral cDNA expression vectors expressing iBMF, iFOXO3 and iFOXO3.A3 were generated using Gateway cloning in the pINDUCER20 Dox-inducible expression system.<sup>50</sup> Guide RNAs for *Cdh1.1* and *Cdh1.2* CRISPR were cloned into the lentiviral pSicoR CRISPR/Cas9 vector<sup>51</sup> using *BsmBI* restriction sites (Supplementary Table S1). After lentiviral transduction, cells were selected for incorporation using puromycin and subsequently FACS-sorted based on E-cadherin expression (DECMA-1, 1 : 2000; Abcam no. 11512, Cambridge, UK). BMF and BIM knockdown in *Trp53<sup>Δ/Δ</sup>-4* cells was achieved by lentiviral transduction of pLKO1-shBMF (TRCN000009716 (shBMF #1) and TRCN000009717 (shBMF #2)) and pLKO1-shBIM (TRCN0000231244 (shBIM #1) and TRCN0000231246 (shBIM #2)), Sigma-Aldrich, Zwijndrecht, The Netherlands), followed by puromycin selection. For MCF7, siRNA smartpools targeting BMF, BIM or control siRNA (Dharmacon M-004393-04-0005 and M-004383-02-0005, Lafayette, CO, USA) were reverse-transfected using HiPerfect (Qiagen, Venlo, The Netherlands) at a final siRNA concentration of 40 nM. Forty-eight hours after transfection, cells were harvested and seeded for anoikis assays.<sup>50,51</sup>

**Immunoblotting and antibodies.** Proteins were detected using SDS-PAGE and subsequent western blotting analysis with primary antibodies recognising BAD (CST-9292, Cell Signaling Technology, Leiden, The Netherlands), BIM (CST-2819), BMF (human: CST-5889, mouse: ENZO-17A9), BID (SC-11423 Santa Cruz, Heidelberg, Germany), AKT/PKB (CST), FOXO1 (CST-29H4), FOXO3 (H144 Santa Cruz), NOXA (SP7122p Acris, Herford, Germany), PUMA (CST-4976) and BCL2 (CST-2876) used at 1 : 2000. Primary antibodies were detected by secondary

HRP-conjugated antibodies targeting mouse, rabbit and rat IgG and visualised using chemiluminescence (Bio-Rad, Veenendaal, The Netherlands).

**Immunofluorescence.** Cells were grown on glass coverslips, fixed using ice-cold methanol and blocked with 2% BSA (Invitrogen, Breda, The Netherlands) and 0.1% normal goat serum (Invitrogen). Cells were stained with mouse anti-p120 (BD616134, 1 : 500 overnight), Alexa Fluor 555-conjugated mouse anti-E-cadherin, (1 : 200, BD560064, 2 h at room temperature) and DAPI (Sigma-Aldrich). Secondary 563-conjugated goat anti-mouse antibodies were used for visualisation on a Zeiss LSM700 confocal microscope (Sliedrecht, The Netherlands).

**Quantitative real-time PCR.** mRNA was isolated from live cells using the Qiagen RNeasy Kit (Qiagen). cDNA synthesis was performed using the iScript cDNA Synthesis Kit (Bio-Rad). Real-time PCR was performed using SYBR green FastStart master mix (Roche, Woerden, The Netherlands) in the CFX Connect Real-time PCR detection system (Bio-Rad). Target genes were amplified using the specific primer pairs (Supplementary Table S1), and specificity was confirmed by analysis of the melting curves. Target gene expression levels were normalised to *GAPDH*, *PBDG* and *TUBA1A* levels.

**Anoikis assays.** Anoikis resistance was analysed by seeding six-well ultra-low cluster polystyrene culture dishes (Corning, Corning, NY, USA) with 50 000 cells/ml. After 24 h, cells were harvested and resuspended in 100 ml of Annexin-V buffer supplemented with Annexin-V (IQ Products, Groningen, The Netherlands) and propidium iodide (Sigma-Aldrich). Anoikis was defined as the Annexin-V and propidium iodide-positive population and quantified using a FACSCalibur (BD Biosciences, Breda, The Netherlands).

**Chromatin immunoprecipitation.** MCF7-iFOXO3 cells were grown under adherent (Ad) or suspension (Sus) conditions in the absence or presence of Dox and treated with the allosteric AKT inhibitor VIII 1 h prior to harvesting to ensure full FOXO activation. Immunoprecipitations were performed on  $20 \times 10^6$  cells with 5  $\mu$ g rabbit anti-FOXO3 (Santa Cruz H144) and 5  $\mu$ g of normal rabbit IgG (Santa Cruz). ChIPs were performed as previously described.<sup>52</sup>

**Orthotopic transplantations and tumour watch.** For longitudinal tumour growth and dissemination experiments, 10 000 *mLc1* cells were transplanted in the fourth inguinal mouse mammary gland of Nude-recipient mice as described previously.<sup>26</sup> Primary tumours were allowed to develop to a volume of 100 mm<sup>3</sup> at which point expression of BMF was induced by feeding Dox-containing chow (Ssniff, Soest, Germany). Alternatively, BMF expression was induced when lung metastasis were detected using BLI of the thorax ( $> 2 \times 10^3$  photons/s/cm<sup>2</sup>/sr). Tumour volumes and lung metastases were followed in time as described using a Biospace  $\phi$  imager (Nesles la Vallée, France).<sup>26</sup> All animal experiments were approved by the Utrecht University Animal Experimental Committee (DEC-ABC no. 2012.III.05.044).

## Conflict of Interest

The authors declare no conflict of interest.

**Acknowledgements.** We thank S Elledge from the HHMI Boston and R Lebbink of the Molecular Microbiology Department, UMC, Utrecht for kindly providing the pINDUCER20 and pSicoR CRISPR/Cas9 constructs and the UMC Utrecht Cell Biology Department for help with confocal imaging. The Derksen, van Diest, Dansen and Burgering laboratories are acknowledged for support and suggestions. Research was supported by grants from the Netherlands Organization for Scientific Research (NWO/ZonMW-VIDI 016.096.318), Foundation Vrienden UMC Utrecht (11.081) and the Dutch Cancer Society (KWF-UU-2011-5230 and KWF-UU-2009-4490).

1. Frisch SM, Screaton RA. Anoikis mechanisms. *Curr Opin Cell Biol* 2001; **13**: 555–562.
2. Schwartz MA. Integrins, oncogenes, and anchorage independence. *J Cell Biol* 1997; **139**: 575–578.
3. Humphreys RC, Krajewska M, Krnacik S, Jaeger R, Weiher H, Krajewski S *et al*. Apoptosis in the terminal endbud of the murine mammary gland: a mechanism of ductal morphogenesis. *Development* 1996; **122**: 4013–4022.

4. Debnath J, Mills KR, Collins NL, Reginato MJ, Muthuswamy SK, Brugge JS. The role of apoptosis in creating and maintaining luminal space within normal and oncogene-expressing mammary acini. *Cell* 2002; **111**: 29–40.
5. Schmelzle T, Mailleux AA, Overholtzer M, Carroll JS, Solimini NL, Lightcap ES *et al*. Functional role and oncogene-regulated expression of the BH3-only factor Bmf in mammary epithelial anoikis and morphogenesis. *Proc Natl Acad Sci USA*. 2007; **104**: 3787–3792.
6. Mailleux AA, Overholtzer M, Schmelzle T, Bouillet P, Strasser A, Brugge JS. Bim regulates apoptosis during mammary ductal morphogenesis, and its absence reveals alternative cell death mechanisms. *Dev Cell* 2007; **12**: 221–234.
7. Westphal D, Dewson G, Czabotar PE, Kluck RM. Molecular biology of Bax and Bak activation and action. *Biochim Biophys Acta* 2011; **1813**: 521–531.
8. Strasser A, Cory S, Adams JM. Deciphering the rules of programmed cell death to improve therapy of cancer and other diseases. *EMBO J* 2011; **30**: 3667–3683.
9. Hausmann M, Leucht K, Ploner C, Kiessling S, Villunger A, Becker H *et al*. BCL-2 modifying factor (BMF) is a central regulator of anoikis in human intestinal epithelial cells. *J Biol Chem* 2011; **286**: 26533–26540.
10. Puthalakath H, Villunger A, O'Reilly LA, Beaumont JG, Coultas L, Cheney RE *et al*. Bmf: a proapoptotic BH3-only protein regulated by interaction with the myosin V actin motor complex, activated by anoikis. *Science* 2001; **293**: 1829–1832.
11. Chiarugi P, Giannoni E. Anoikis: a necessary death program for anchorage-dependent cells. *Biochem Pharmacol* 2008; **76**: 1352–1364.
12. Muthuswamy SK, Li D, Lelievre S, Bissell MJ, Brugge JS. ErbB2, but not ErbB1, reinitiates proliferation and induces luminal repopulation in epithelial acini. *Nat Cell Biol* 2001; **3**: 785–792.
13. Danes CG, Wyszomierski SL, Lu J, Neal CL, Yang W, Yu D. 14-3-3 zeta down-regulates p53 in mammary epithelial cells and confers luminal filling. *Cancer Res* 2008; **68**: 1760–1767.
14. Samuels Y, Wang Z, Bardelli A, Silliman N, Ptak J, Szabo S *et al*. High frequency of mutations of the PIK3CA gene in human cancers. *Science* 2004; **304**: 554.
15. Datta SR, Dudek H, Tao X, Masters S, Fu H, Gotoh Y *et al*. Akt phosphorylation of BAD couples survival signals to the cell-intrinsic death machinery. *Cell* 1997; **91**: 231–241.
16. Gardai SJ, Hildeman DA, Frankel SK, Whitlock BB, Frasch SC, Borregaard N *et al*. Phosphorylation of Bax Ser184 by Akt regulates its activity and apoptosis in neutrophils. *J Biol Chem* 2004; **279**: 21085–21095.
17. Qian X, Karpova T, Sheppard AM, McNally J, Lowy DR. E-cadherin-mediated adhesion inhibits ligand-dependent activation of diverse receptor tyrosine kinases. *EMBO J* 2004; **23**: 1739–1748.
18. Schackmann RCJ, Klarenbeek S, Vlugg EJ, Stelloo S, van Amersfoort M, Tenhagen M *et al*. Loss of p120-catenin induces metastatic progression of breast cancer by inducing anoikis resistance and augmenting growth factor receptor signaling. *Cancer Res* 2013; **73**: 4937–4949.
19. van Roy F, Bex G. The cell-cell adhesion molecule E-cadherin. *Cell Mol Life Sci* 2008; **65**: 3756–3788.
20. Derksen PWB, Braumuller TM, van der Burg E, Hornsveld M, Mesman E, Wesseling J *et al*. Mammary-specific inactivation of E-cadherin and p53 impairs functional gland development and leads to pleomorphic invasive lobular carcinoma in mice. *Dis Models Mech* 2011; **4**: 347–358.
21. Boussadia O, Kutsch S, Hierholzer A, Delmas V, Kemler R. E-cadherin is a survival factor for the lactating mouse mammary gland. *Mech Dev* 2002; **115**: 53–62.
22. Bex G, van Roy F. Involvement of members of the cadherin superfamily in cancer. *Cold Spring Harb Perspect Biol* 2009; **1**: a003129.
23. Derksen PWB, Liu X, Saridin F, van der Gulden H, Zevenhoven J, Evers B *et al*. Somatic inactivation of E-cadherin and p53 in mice leads to metastatic lobular mammary carcinoma through induction of anoikis resistance and angiogenesis. *Cancer Cell* 2006; **10**: 437–449.
24. Vaillant F, Merino D, Lee L, Breslin K, Pal B, Ritchie ME *et al*. Targeting BCL-2 with the BH3 mimetic ABT-199 in estrogen receptor-positive breast cancer. *Cancer Cell* 2013; **24**: 120–129.
25. Muranen T, Selfors LM, Worster DT, Iwanicki MP, Song L, Morales FC *et al*. Inhibition of PI3K/mTOR leads to adaptive resistance in matrix-attached cancer cells. *Cancer Cell* 2012; **21**: 227–239.
26. Schackmann RCJ, van Amersfoort M, Haarhuis JHI, Vlugg EJ, Halim VA, Roodhart JML *et al*. Cytosolic p120-catenin regulates growth of metastatic lobular carcinoma through Rock1-mediated anoikis resistance. *J Clin Invest* 2011; **121**: 3176–3188.
27. Reginato MJ, Mills KR, Becker EB, Lynch DK, Bonni A, Muthuswamy SK *et al*. Bim regulation of lumen formation in cultured mammary epithelial acini is targeted by oncogenes. *Mol Cell Biol* 2005; **25**: 4591–4601.
28. Eijkelenboom A, Burgering BMT. FOXOs: signalling integrators for homeostasis maintenance. *Nat Rev Mol Cell Biol* 2013; **14**: 83–97.
29. Brunet A, Bonni A, Zigmond MJ, Lin MZ, Juo P, Hu LS *et al*. Akt promotes cell survival by phosphorylating and inhibiting a Forkhead transcription factor. *Cell* 1999; **96**: 857–868.
30. Hanahan D, Weinberg RA. Hallmarks of cancer: the next generation. *Cell* 2011; **144**: 646–674.
31. Curto M, Cole BK, Lallemand D, Liu CH, McClatchey AI. Contact-dependent inhibition of EGFR signaling by Nf2/Merlin. *J Cell Biol* 2007; **177**: 893–903.
32. Juin P, Geneste O, Gautier F, Depil S, Campone M. Decoding and unlocking the BCL-2 dependency of cancer cells. *Nat Rev Cancer* 2013; **13**: 455–465.
33. Eijkelenboom A, Mokry M, de Wit E, Smits LM, Polderman PE, van Triest MH *et al*. Genome-wide analysis of FOXO3 mediated transcription regulation through RNA polymerase II profiling. *Mol Syst Biol* 2013; **9**: 638.
34. Eijkelenboom A, Mokry M, Smits LM, Nieuwenhuis EE, Burgering BMT. FOXO3 selectively amplifies enhancer activity to establish target gene regulation. *Cell Rep* 2013; **5**: 1664–1678.
35. Zhang Y, Adachi M, Kawamura R, Imai K. Bmf is a possible mediator in histone deacetylase inhibitors FK228 and CBHA-induced apoptosis. *Cell Death Differ* 2006; **13**: 129–140.
36. Shao Y, Aplin AE. BH3-only protein silencing contributes to acquired resistance to PLX4720 in human melanoma. *Cell Death Differ* 2012; **19**: 2029–2039.
37. VanBroeklin MW, Verhaegen M, Soengas MS, Holmen SL. Mitogen-activated protein kinase inhibition induces translocation of Bmf to promote apoptosis in melanoma. *Cancer Res* 2009; **69**: 1985–1994.
38. Shao Y, Aplin AE. ERK2 phosphorylation of serine 77 regulates Bmf pro-apoptotic activity. *Cell Death Dis* 2012; **3**: e253.
39. Bolden JE, Shi W, Jankowski K, Kan CY, Cluse L, Martin BP *et al*. HDAC inhibitors induce tumor-cell-selective pro-apoptotic transcriptional responses. *Cell Death Dis* 2013; **4**: e519.
40. Chen J, Gomes AR, Monteiro LJ, Wong SY, Wu LH, Ng T-T *et al*. Constitutively nuclear FOXO3a localization predicts poor survival and promotes Akt phosphorylation in breast cancer. *PLoS One* 2010; **5**: e12293.
41. Piñon JD, Labi V, Egle A, Villunger A. Bim and Bmf in tissue homeostasis and malignant disease. *Oncogene* 2008; **27 Suppl 1**: S41–S52.
42. Labi V, Erlacher M, Kiessling S, Manzi C, Frenzel A, O'Reilly L *et al*. Loss of the BH3-only protein Bmf impairs B cell homeostasis and accelerates gamma irradiation-induced thymic lymphoma development. *J Exp Med* 2008; **205**: 641–655.
43. Chonghaile TN, Roderick JE, Glenfield C, Ryan J, Sallan SE, Silverman LB *et al*. Maturation stage of T-cell acute lymphoblastic leukemia determines BCL-2 versus BCL-XL dependence and sensitivity to ABT-199. *Cancer Discov* 2014; **4**: 1074–1087.
44. Miller LA, Goldstein NB, Johannes WU, Walton CH, Fujita M, Norris DA *et al*. BH3 mimetic ABT-737 and a proteasome inhibitor synergistically kill melanomas through Noxa-dependent apoptosis. *J Invest Dermatol* 2009; **129**: 964–971.
45. Choudhary GS, Al-Harbi S, Mazumder S, Hill BT, Smith MR, Bodo J *et al*. MCL-1 and BCL-XL-dependent resistance to the BCL-2 inhibitor ABT-199 can be overcome by preventing PI3K/AKT/mTOR activation in lymphoid malignancies. *Cell Death Dis* 2015; **6**: e1593.
46. Reuland SN, Goldstein NB, Partyka KA, Cooper DA, Fujita M, Norris DA *et al*. The combination of BH3-mimetic ABT-737 with the alkylating agent temozolomide induces strong synergistic killing of melanoma cells independent of p53. *PLoS One* 2011; **6**: e24294.
47. Oakes SR, Vaillant F, Lim E, Lee L, Breslin K, Feleppa F *et al*. Sensitization of BCL-2-expressing breast tumors to chemotherapy by the BH3 mimetic ABT-737. *Proc Natl Acad Sci USA* 2012; **109**: 2766–2771.
48. Kutuk O, Letai A. Displacement of Bim by Bmf and Puma rather than increase in Bim level mediates paclitaxel-induced apoptosis in breast cancer cells. *Cell Death Differ* 2010; **17**: 1624–1635.
49. Mukherjee N, Reuland SN, Lu Y, Luo Y, Lambert K, Fujita M *et al*. Combining a BCL2 inhibitor with the retinoid derivative fenretinide targets melanoma cells including melanoma initiating cells. *J Invest Dermatol* 2015; **135**: 842–850.
50. Meerbrey KL, Hu G, Kessler JD, Roarty K, Li MZ, Fang JE *et al*. The pINDUCER lentiviral toolkit for inducible RNA interference in vitro and in vivo. *Proc Natl Acad Sci USA* 2011; **108**: 3665–3670.
51. van de Weijer ML, Bassik MC, Luteijn RD, Voorburg CM, Lohuis MA, Kremmer E *et al*. A high-coverage shRNA screen identifies TMEM129 as an E3 ligase involved in ER-associated protein degradation. *Nat Commun* 2014; **5**: 3832.
52. Renault VM, Thekkat PU, Hoang KL, White JL, Brady CA, Kenzelmann Broz D *et al*. The longevity gene FoxO3 is a direct target of the p53 tumor suppressor. *Oncogene* 2011; **30**: 3207–3221.

Supplementary Information accompanies this paper on Cell Death and Differentiation website (<http://www.nature.com/cdd>)